particle inclsive cross sections, where the crossover with the p_T^{-4} terms is at $p_T \approx 7$ GeV. See Ref. 6. We have used $\alpha_M = 1.2$ GeV^2 from Ref. 9.

[11]There are additional CIM $p_\perp^{-8}$ contributions from $q\bar{q} \to M\bar{M}$, etc., which behaves as $p_T^{-8}(1-x_R)^3$ and dominates Eq. (11) at large x_R.

[12]No double counting occurs when we include all these subprocesses in the jet cross section. The different terms are distinct contributions to the cross section with unique topologies of jets and quark charge structures. Nor are we double counting when we include both $\gamma\gamma \to q\bar{q}$ and vector-dominated $\gamma\gamma \to M\bar{M} \to q\bar{q}$, as long as we include only a sum over a finite number of vector mesons M; in fact, the different p_T behaviors of the cross sections make differentiation between these subprocesses clear.

Confirmation of Exchange-Degeneracy Predictions in the Line-Reversed Reactions: $\pi^+p \to K^+Y^*(1385)$ and $K^-p \to \pi^-Y^*(1385)$ at 11.5 GeV/c

J. Ballam, J. Bouchez,[a] J. T. Carroll, C. V. Cautis, G. B. Chadwick, V. Chaloupka, R. C. Field, D. R. Freytag, R. A. Lewis,[b] M. N. Minard, K. C. Moffeit, and R. A. Stevens

Stanford Linear Accelerator Center, Stanford University, Stanford, California 94305

(Received 5 July 1978)

We have measured in a single experimental setup the differential cross sections and polarizations of the $Y^*(1385)$ produced in the two line-reversed reactions $\pi^+p \to K^+Y^*(1385)$ (260 eV/μb) and $K^-p \to \pi^-Y^*(1385)$ (180 eV/μb) at 11.5 GeV/c. We compare these results to Σ^+ production in the same experiment. The data have been derived from a triggered bubble-chamber experiment using the SLAC Hybrid Facility. We find that both helicity-flip–dominated (Y^*) and helicity-nonflip–dominated (Σ) processes are consistent with weak–exchange-degeneracy predictions.

As part of a systematic study of line reversal in hypercharge-exchange reactions, we present here results on $Y^*(1385)$ production in the reactions

$$\pi^+p \to K^+Y^*(1385), \qquad (1)$$

$$K^-p \to \pi^-Y^*(1385), \qquad (2)$$

at 11.5-GeV/c incoming momentum. In a Regge picture, the two reactions are expected to be dominated asymptotically by the exchange of the same two reggeons: the vector $K^*(890)$ and tensor $K^{**}(1420)$. Exchange degeneracy (EXD) of these trajectories implies equal cross sections for reactions (1) and (2) at the same value of the four-momentum transfer, t. The polarization of the final-state hyperon should be either zero (strong EXD) or, if different from zero, it should have equal magnitude and opposite sign (weak EXD) in line-reversed reactions.[1] Our experiment was designed to test these relations.

Previous measurements of reactions (1) and (2) have mostly resulted from experiments done by different groups using different techniques,[2-4] thus making comparisons difficult to interpret. The present experiment is the first one to measure in a single detector the complete decay angular distribution of the $Y^*(1385)$ for both reactions (1) and (2), from which we determine the hyperon polarization. We also measure the differential cross sections of the two reactions with a minimum of systematic differences between them. For comparison, we present differential cross sections and hyperon polarizations from the reactions

$$\pi^+p \to K^+\Sigma^+, \qquad (3)$$

$$K^-p \to \pi^-\Sigma^+. \qquad (4)$$

The Σ polarization results presented here include new data in addition to those presented in an earlier publication.[5] The experiment was conducted at the SLAC Hybrid Facility[6] consisting of the SLAC 1-m rapid-cycling bubble chamber (15 Hz), triggered by data from electronic detectors processed on line by a DGC-840 computer. The experimental setup and the trigger and described elsewhere.[5,6]

Events belonging to reactions (1)–(4) have been identified by kinematic fits, simultaneously at both primary and strange-particle decay vertices. For reactions (1) and (2), the mass resolution of constrained events is ~8 MeV in the $Y^*(1385)$ region.

The resulting sample is almost bias free and has well-understood relative normalizations for all reactions. The data in both exposures have been corrected for (a) fast-trigger dead time, (b) proportional wire chamber inefficiencies, (c) software trigger losses, (d) interaction or decay of the incident beam, (e) interaction or decay of the triggering particle, (f) random scanning and measurement losses, (g) strange-particle decays too close or too far from the primary vertex. In addition, the K^- exposure was corrected for the hadron punchthrough in the μ hodoscope and the π^+ exposure for μ contamination in the beam and for pion pileup in the downstream Cherenkov counter. The overall systematic uncertainty in our normalization is ±10%.

The detector has ~100% acceptance in the interval $0.01 < -t < 1$ GeV^2. We have corrected all distributions for the loss of events with $-t < 0.01$ GeV^2 due to the triggering algorithm. In addition, we found small losses in the Λ sample which bias some of the angular distributions: Asymmetric vees in which one of the tracks (mostly π^-) is too short to be properly measured or vees which do not open up sufficiently at the decay vertex and are misidentified as γ conversions. These losses amount to $\lesssim 3\%$ and have been taken into account when fitting angular distributions. The scanning loss in $\Sigma^+ \to p\pi^0$ has also been taken into account when measuring Σ^+ polarization.[5]

The present analysis is based on the sample of events described in Table I. We have made a model-independent analysis of $Y^*(1385)$ production in reactions (1) and (2). The variables which we choose to describe the four-particle final state are as follows: t, square of four-momentum transfer to the fast forward particles (K^+ or π^-); $m_{\Lambda\pi^+}$, invariant mass of the $\Lambda\pi^+$ system; and Ω, a set of four angles describing the cascade decay $Y^* \to \Lambda\pi^+$, $\Lambda \to p\pi^-$.[3]

We used the extended maximum-likelihood method[7] to separate $Y^*(1385)$ production as function of momentum transfer. All cuts imposed on the experimental sample were taken into account in the theoretical expressions. After each fit we have plotted the result of the fit on top of different experimental distributions and found good agreement with the data. The method of analysis, the variables used, and the parametrization of the $Y^*(1385)$ are similar to those used by Holmgren *et al.*[3] The maximization of the log-likelihood function was done using the program OPTIME.[8]

The invariant-mass distribution of the $\Lambda\pi^+$ system from both reactions (1) and (2) show a prominent peak due to $Y^*(1385)$ production, over a background level less than 10% of the signal (see Fig. 1). There is also some accumulation of events at higher mass, primarily due to the $Y^*(1670)$ isobar. To obtain a good description of the mass spectrum up to 2 GeV, we tried several parametrizations for the background. We obtained the best fit with a p-wave Breit-Wigner function[9] for the $Y^*(1385)$ and two simple Breit-Wigner functions in the $m_{\Lambda\pi} \sim 1.7$ GeV region, plus a constant phase-space term.

The results for the $Y^*(1385)$ did not depend on the parametrization used for the background.

TABLE I. Statistics and cross sections. The integrated cross sections correspond to the interval $-t < 1$ GeV^2. The parameters A_1, A_2, and b have been determined from fits according to Eq. (5) in the interval $-t < 0.4$ GeV^2 for the Σ reactions and $-t < 1$ GeV^2 for the $Y^*(1385)$ reactions.

Reaction	Events	Sensitivity (eV/μb)	Cross section[a] (μb)	A_1[b] (μb/GeV^2)	A_2[b] (μb/GeV^4)	b[b] (GeV^{-2})
$\pi^+p \to K^+\Sigma^+$, $\Sigma^+ \to p\pi^0$	1086	260.1	23.1 ± 2.4	246 ± 12	0	10.5 ± 0.4
$\pi^+p \to K^+\Sigma^+$, $\Sigma^+ \to n\pi^+$	1232					
$K^-p \to \pi^-\Sigma^+$, $\Sigma^+ \to p\pi^0$	715	180.2	27.0 ± 2.9	236 ± 13	0	9.8 ± 0.4
$K^-p \to \pi^-\Sigma^+$, $\Sigma^+ \to n\pi^+$	962					
$\pi^+p \to K^+Y^*(1385)$	936	260.1	7.0 ± 0.8	10 ± 3	326 ± 25	7.0 ± 0.4
$K^-p \to \pi^-Y^*(1385)$	911	180.2	10.1 ± 1.1	13 ± 3	362 ± 28	

[a]Error includes 10% systematic uncertainty. [b]Statistical errors only.

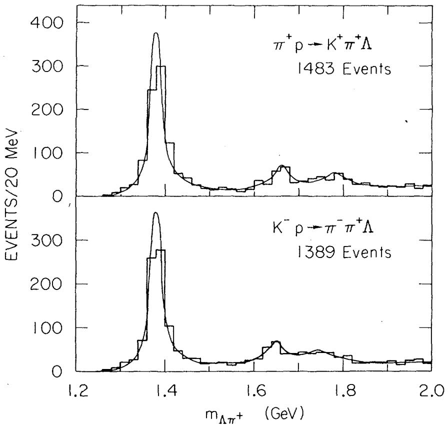

FIG. 1. Invariant-mass distribution of the $\Lambda\pi^+$ system. The solid line is the result of the maximum-likelihood fit.

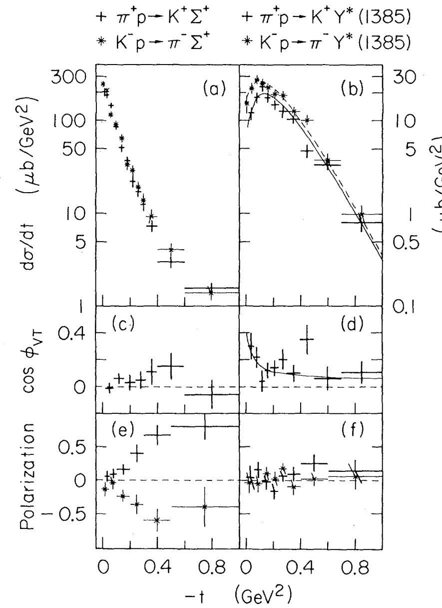

FIG. 2. Comparison of differential cross sections and hyperon polarizations for the two pairs of line-reversed reactions (1)–(4). (a), (b) Differential cross sections. The Y^* cross sections refer to the scale on the right. The lines are results of fits described in the text. The solid line is the fit to the π^+ data and the dashed one to the K^- data. (c), (d) Cross section asymmetry

$$\langle\cos\varphi_{VT}\rangle = \frac{d\sigma/dt(K^-) - d\sigma/dt(\pi^+)}{d\sigma/dt(K^-) + d\sigma/dt(\pi^+)}.$$

The solid line has been calculated using the results of fits to the differential cross sections. (e), (f) Hyperon polarization along the normal to the production plane.

The parameters of the $Y^*(1385)$ and the high-mass enhancements were determined from fits in the region $m_{\Lambda\pi^+} < 2$ GeV and $-t < 1$ GeV^2. We find the mass and width of the $Y^*(1385)$ to be consistent within errors in the π^+ and K^- reactions. In the final fits we used the average values $m_0 = 1.380 \pm 0.002$ GeV and $\Gamma = 0.030 \pm 0.004$ GeV.

With the mass and width of the $Y^*(1385)$ fixed, we have measured the differential cross sections by fitting the amount of resonance production in several t intervals up to $-t = 1$ GeV^2. The cross sections for reactions (1) and (2) have been corrected for the $Y^*(1385) \to \Lambda\pi$ and $\Lambda \to p\pi^-$ decay branching ratios (0.88 and 0.642, respectively). The results are shown in Figs. 2(a) and 2(b), together with the differential cross sections from reactions (3) and (4). Only the decay $\Sigma^+ \to n\pi^+$ has been used in Fig. 2(a), to reduce systematic uncertainties.

The Σ^+ differential cross sections show a simple exponential slope with some indication of flattening off for $-t > 0.4$ GeV^2. The $Y^*(1385)$ cross sections show a forward dip, suggesting that the Y^* vertex (as opposed to the Σ vertex) is helicity-flip dominated.

The Σ^+ differential cross sections are nearly equal in slope and relative normalization while the $Y^*(1385)$ show significant differences at small $|t|$. Most of the difference between the Y^* cross sections is of kinematic origin: Angular momentum conservation forces the helicity-flip–dominated cross section to go to zero at $\langle t_{min}\rangle = -0.012$ GeV^2 in reaction (1), and at $\langle t_{min}\rangle \simeq +0.011$ GeV^2 in reaction (2), thus yielding different cross sections at small $|t|$.

To describe this effect quantitatively, we did minimum-χ^2 fits to the differential cross sections using the function

$$\frac{d\sigma}{dt} = [A_1 - A_2(t - t_{min})]e^{bt}, \qquad (5)$$

where A_1 and A_2 approximate the helicity-nonflip and -flip contributions, respectively. For the Y^* reactions the slopes of the differential cross sections were equal within errors, so that for the final fits we fixed them to the same value. The fits give a good description of the data as shown in Fig. 2(b). In particular, the turnover at low t is well described by Eq. (5), confirming thus the kinematic origin of the difference in cross sections at low $|t|$ between reactions (1) and (2).

The values of A_1 and A_2 (see Table I) indicate that, within the limits of systematic uncertainties in this experiment, the data are in agreement with EXD predictions for both pairs of line-reversed reactions. (Note that the errors quoted in Table I are statistical only.)

To express quantitatively the difference between the K^-- and π^+-induced reactions, we plot in Figs. 2(c) and 2(d) the ratio

$$\langle\cos\varphi_{VT}\rangle = \frac{d\sigma(K^-)/dt - d\sigma(\pi^+)/dt}{d\sigma(K^-)/dt + d\sigma(\pi^+)/dt} \qquad (6)$$

as function of $-t$. For small $|t|$ this quantity is a measure of the phase difference between the vector and tensor amplitudes[10] and EXD predicts $\varphi_{VT} = \pi/2$. Apart from the rise at low $|t|$ in the Y^* reactions, the data are consistent with this value. The solid line in Fig. 2(d) has been calculated from the fits shown in Fig. 2(b).

Using A_1 as a representative value for the Σ cross section and A_2 for the Y^*, we calculate $\langle\cos\varphi_{VT}\rangle = 0.05 \pm 0.10$ for reactions (1) and (2) and $\langle\cos\varphi_{VT}\rangle = -0.02 \pm 0.10$ for reactions (3) and (4). The quoted errors include the maximum systematic difference possible between the π^+ and K^- samples.

The only other experiment which has previously studied both pairs of reactions in a single experimental setup is a missing-mass experiment at 10.1 GeV/c.[4] They found in their experiment that reactions (1) and (2) violate EXD predictions while reactions (3) and (4) are in approximate agreement. Our data show that most of the differences between both pairs of line-reversed reactions are of kinematic origin. Apart from kinematic differences, the cross sections for both helicity-flip–dominated (Y^*) and helicity-nonflip–dominated (Σ) processes are in good agreement with EXD predictions.

To measure the spin polarization of the final-state hyperon, we have analyzed the decay angular distributions of the Σ^+ and of the cascade process $Y^*(1385) \to \Lambda\pi^+$, $\Lambda \to p\pi^-$. The Σ^+ analysis has been described elsewhere[5] and the result is shown in Fig. 2(e). For the $Y^*(1385)$ we have estimated density-matrix elements (ρ_{mm}) by fitting the decay angular distribution of the Y^* in the transversity frame.[11] We summarize our results in Fig. 2(f) by plotting the Y^* polarization defined as $PJ^{-1}\sum m\rho_{mm}$ where m is the spin projection of the Y^* along the normal to the production plane. The Σ^+ polarization is consistent with weak-EXD predictions while the $Y^*(1385)$ has a polarization consistent with zero over the entire t range for both reactions (1) and (2). This agrees with strong EXD: However, the Stodolsky-Sakurai[12] or additive quark models[13] predict the same behavior.

In conclusion, our data for two pairs of line-reversed, hypercharge-exchange reactions are consistent with exchange-degeneracy predictions for both helicity-flip and -nonflip amplitudes.

This work was supported by the U. S. Department of Energy.

---

[a]Present address: Département de Physique de Particules Elémentaires, Centre d'Etudes Nucléaires–Saclay, F-91190 Gif-sur-Yvette, France.

[b]Present address: Physics Department, Michigan State University, East Lansing, Mich. 48824.

[1]K.-W. Lai and J. Louie, Nucl. Phys. B19, 205 (1970).

[2]M. Aderholz *et al.*, Nucl. Phys. B11, 259 (1969); A. Bashian *et al.*, Phys. Rev. D 4, 2667 (1971); M. Aguilar-Benitez *et al.*, Phys. Rev. D 6, 29 (1972); D. Birnbaum *et al.*, Phys. Lett. 31B, 484 (1970); B. Chaurand *et al.*, Nucl. Phys. B117, 1 (1976).

[3]S. O. Holmgren *et al.*, Nucl. Phys. B119, 261 (1977).

[4]A. Berglund *et al.*, Phys. Lett. 60B, 117 (1975), and 73B, 369 (1978).

[5]P. A. Baker *et al.*, Phys. Rev. Lett. 40, 678 (1978).

[6]G. B. Bowden *et al.*, Nucl. Instrum. Methods 138, 75 (1976); J. Ballam and R. Watt, Annu. Rev. Nucl. Sci. 27, 75 (1977); R. C. Field, SHF Memo 67, Internal Publication SLAC, Group BC, 1977 (unpublished).

[7]J. Orear, University of California Research Laboratory Report No. UCRL-8417, 1958 (unpublished).

[8]P. H. Eberhard and W. D. Koellner, Comp. Phys. Commun. 3, 296 (1972), and 5, 163 (1973).

[9]J. D. Jackson, Nuovo Cimento 34, 1644 (1964).

[10]A. C. Irving and R. P. Worden, Phys. Rep. 34C, 117 (1977).

[11]The normal to the production plane is defined as $\vec{n} = \vec{B} \times \vec{M}$ where $\vec{B}$ is the beam direction and $\vec{M}$ is the direction of the particle recoiling against the Y^* or Σ.

[12]L. Stodolsky and J. J. Sakurai, Phys. Rev. Lett. 11, 90 (1963).

[13]A. Bialas and K. Zalewski, Nucl. Phys. B6, 449 (1968).